*J. Fluid Mech.* (1985), *vol.* 159, *pp.* 175–193
*Printed in Great Britain*



# Compressible-flow channel flutter

By J. B. GROTBERG† AND T. R. SHEE
Department of Engineering Sciences and Applied Mathematics, The Technological Institute, Northwestern University, Evanston, Illinois 60201

(Received 17 December 1984 and in revised form 15 April 1985)

The effect of fluid compressibility on the dynamic stability of a two-dimensional flow through a flexible channel is analysed. The compressibility parameter $Q$ is defined as the ratio of a reference elastic wave speed of the wall to the local speed of sound. As the fluid speed increases, the walls become dynamically unstable at the critical fluid speed $S_0$ and start to flutter at critical frequency $\omega_0$. The effect of three other dimensionless parameters on the critical condition is also analysed. These are the ratio $\gamma$ of fluid damping to wall damping, the ratio $B$ of wall bending resistance to elastance, and the ratio $\mu$ of wall to fluid mass. Nonlinear analysis using the Poincaré–Lindstedt method shows stiffening at supercritical speeds. Further stability analysis using the method of multiple scales shows that the amplitude growth is finite and the nonlinear fluttering state is stable. Both symmetric and antisymmetric modes of oscillation are analysed. A frictionless system is found to be a singular case in the nonlinear theory. The hydraulic approximation employed in the analysis is shown to be a particular limiting form of the corresponding Orr–Sommerfeld system.

## 1. Introduction

The study of flow through flexible tubes has received impetus from its application to a variety of physical situations ranging from strictly engineering contexts to biomedical phenomena (Grotberg & Davis 1980; Gavriely *et al.* 1984). The conveyed fluids of interest include both gases and liquids, while their surrounding conduits can have the rigidity of metals or the softness of biological tissue. Grotberg & Reiss (1984) have previously investigated incompressible flow through a flexible two-dimensional channel, and showed that, in the presence of wall damping, flutter instability occurs only when fluid damping is included in the model. The predictions of this theory depend on several parameters, including the fluid speed $U$ and the wall elastic speed $C$. Modelling the flow as incompressible assumes that the sound speed $a$ is much larger than either of these two characteristic speeds, i.e.

$$Q = \frac{C}{a} \ll 1, \quad M = \frac{U}{a} \ll 1. \tag{1.1}$$

This assumption is not justified in general, because the variety of physical applications includes parameter ranges where either $Q$ or $M$ or both are not negligible.

Flow of a compressible fluid over one side of a single flexible surface has been examined by Dowell (1967) with regard to aeronautical applications of panel flutter.

† Also at Department of Anesthesia, Northwestern University Medical School, 303 East Chicago Avenue, Chicago, Illinois 60611.

His theory for a three-dimensional plate, simply supported on all sides, employs inviscid potential-flow theory and von Kármán's large-deflection plate equation. That theory predicts flutter instability for supersonic flows, $M > 1$, but static divergence instability for subsonic flows, $M < 1$. In a later paper, Matsuzaki & Fung (1979) examined the static divergence of a two-dimensional flexible channel section, initially treating the full compressible-fluid effects but neglecting fluid viscosity. Their analysis is eventually simplified, however, by ignoring terms of order $M^2$ (which discards any contributions from compressibility) in their scaled mass-conservation equation. Consequently, the question of how sound speed affects the static stability of their system, which is raised early in the paper, remains to be answered.

We develop in §2 an analysis of viscous compressible flow through a flexible channel to determine how compressibility alters the dynamic flutter instability discussed in Grotberg & Reiss (1984). The von Kármán nonlinear plate theory is used to model the channel walls, and the fluid damping is modelled by a hydraulic approximation. A complete solution to the coupled fluid and elastic equations would involve a complicated Orr–Sommerfeld system subject to kinematic and stress boundary conditions at the unknown wall position. The difficulty of solving such a problem warrants a simpler approach by employing a hydraulic approximation to model the viscous-fluid effects. We replace the viscous term of the Navier–Stokes equations with a term linearly related to the fluid velocity, $-2f^*u^*$. The consequence of this substitution is discussed in §7, where it is shown that the hydraulic approximation leads to a stability theory that is a particular limit of the full Orr–Sommerfeld system. The linear stability of this fluid–elastic system is studied in §3, where we show that the channel loses stability by flutter. In §4 we employ the Poincaré–Linstedt perturbation method to examine the supercritical bifurcation of flutter states. The stability of these flutter states is established in §5 by solving the initial-value problem using the multitime method, showing that a limit cycle is reached which corresponds to the predictions of §4. The growth rate of the unstable oscillations to the stable limit cycle is examined as a function of compressibility. Section 6 pertains to the frictionless problem and the difficulties that arise when examining the nonlinear theory.

## 2. Problem formulation

Figure 1 shows the infinite channel comprised of parallel flexible plates conveying a viscous compressible fluid. The plates have thickness $h$, bending stiffness $D$, elastance $E$, density $\rho_w$, and linear damping coefficient $g^*$. The channel gap is of average width $2b$ and contains a fluid with unperturbed density $\rho_f$, and sound speed $a$, which flows in the positive-$x$ direction at average speed $U$. For brevity, the governing equations will be presented in dimensionless form. The conversion to dimensional quantities is given in Appendix B.

The continuity equation for the compressible fluid is

$$\nabla^2\Phi - Q^2\left(\frac{\partial}{\partial t}+S\frac{\partial}{\partial x}\right)^2\Phi = 0, \tag{2.1}$$

where $Q = C/a$ and $S = U/C$. Here we have neglected the damping term due to viscosity, since we assumed the quantity $\nu/ab$ is negligibly small. Note that the Mach number is $M = QS$. The velocity potential $\Phi$ satisfies (2.1) subject to the kinematic boundary conditions at the upper and lower walls. These may be simplified by

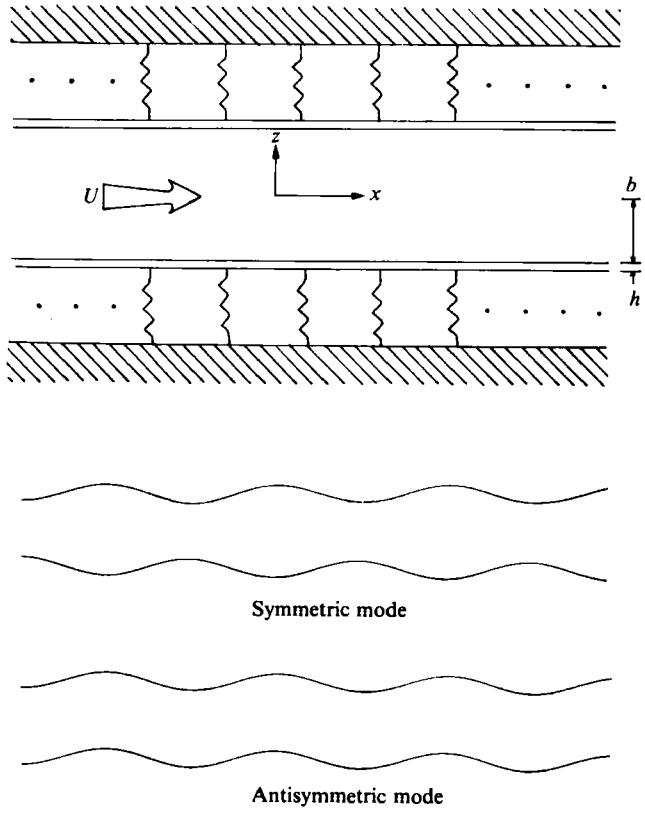


FIGURE 1. An infinite, two-dimensional channel conveying a viscous compressible fluid. Two modes of deformation are shown.

selecting the symmetric mode and antisymmetric mode of disturbances for consideration (see figure 1). The conditions on $\Phi$ at the channel midplane are then

$$\Phi_z = 0, \quad z = 0 \text{ symmetric}, \tag{2.2a}$$

$$\Phi = 0, \quad z = 0 \text{ antisymmetric}, \tag{2.2b}$$

while for either mode the lower wall condition is

$$W_t + \Phi_x W_x - \Phi_z = 0 \quad \text{for } z = W, \tag{2.3}$$

where $W = W(x,t)$ is the unknown position of the lower wall. By solving (2.1)–(2.3), we can, in principle, find $\Phi$ as a function of $W$. The fluid pressure $P$ can be derived from $\Phi$, and hence $W$, by using the unsteady Bernoulli equation,

$$P = P_a - [\Phi_t + \tfrac{1}{2}\nabla\Phi\cdot\nabla\Phi + 2f\Phi], \tag{2.4}$$

which contains the scaled friction factor $f$ as a dimensionless parameter. The steady driving pressure is $P_a$. The final governing equation is the stress boundary condition for the lower plate. Using the one-dimensional von Kármán nonlinear plate equation for periodic disturbances, we have

$$\mu W_{tt} + 2gW_t + BW_{xxxx} + (1+W) - dW_{xx}\int_x^{x+\lambda} (W_x)^2\,dx + P - P_e = 0 \quad \text{for } z = W. \tag{2.5}$$

The dimensionless parameters are (see Appendix B) the ratio $\mu$ of wall mass to fluid mass, the wall damping $g$, the ratio $B$ of bending stiffness to elastance, the coefficient $d$ of nonlinearly induced wall tension and the wavelength $\lambda$ of $x$-periodic disturbances. The external pressure $P_e$ is chosen to keep the undisturbed channel walls parallel. This equilibrium position is at $z = W \equiv -1$, which cancels the spring-loading term of (2.5). By inserting $P$ as a function of $W$ into (2.5), we have reduced the problem to one equation with one unknown variable.

The basic state of (2.1)–(2.5) will be defined as uniform plug flow with Cartesian velocity components $\boldsymbol{u}_0 = \nabla\Phi_0 = (S, 0)$ and constant lower-wall position $W_0 = -1$. The parameter $S$ is our dimensionless speed index scaled on the wall velocity $C$. The friction factor causes a linear pressure drop in the flow direction, $P_{0x} = -2fS$, which must be balanced by $P_e$. It is apparent that $\Phi_0$, $W_0$ and $P_0$ are solutions to the governing equations for all values of the parameter $S$. The formulation of this problem differs from that in Grotberg & Reiss (1984) by the compressibility term in (2.1). The incompressible limit in the present analysis is obtained by setting $Q = 0$.

## 3. Linear stability theory

We study the stability of this system by perturbing it with travelling-wave disturbances that are linearized about the basic-state plug flow. The linear stability theory can be represented in compact form as

$$\mathbf{L}\cdot\boldsymbol{\Psi}_1 = \mathbf{0}, \tag{3.1a}$$

where $\boldsymbol{\Psi}_1$ is a three-component vector,

$$\boldsymbol{\Psi}_1 = \begin{bmatrix} \Phi_1(x,z,t) \\ W_1(x,t) \\ \Phi_1(x,-1,t) \end{bmatrix},$$

and $\mathbf{L}$ is the matrix differential operator

$$\mathbf{L} = \begin{bmatrix} \nabla^2 - Q^2\left(\dfrac{\partial}{\partial t} + S\dfrac{\partial}{\partial X}\right)^2 & 0 & 0 \\ 0 & -\left(\mu\dfrac{\partial^2}{\partial t^2} + 2g\dfrac{\partial}{\partial t} + B\dfrac{\partial^4}{\partial x^4} + 1\right) & \dfrac{\partial}{\partial t} + S\dfrac{\partial}{\partial x} + 2f \\ \dfrac{\partial}{\partial z}(\ )_{z=-1} & -\left(\dfrac{\partial}{\partial t} + S\dfrac{\partial}{\partial x}\right) & 0 \end{bmatrix} \tag{3.1b}$$

subject to the midplane boundary conditions (2.2).

The solution of (3.1) for the symmetric mode has the form

$$\boldsymbol{\Psi}_1 = A \begin{bmatrix} \dfrac{\mathrm{i}(\omega - kS)}{q \sinh q} \cosh qz \\ 1 \\ \dfrac{\mathrm{i}(\omega - kS)}{q \tanh q} \end{bmatrix} \mathrm{e}^{\mathrm{i}\theta} + \text{c.c.}, \tag{3.2}$$

where $\theta = kx - \omega t$, $k = 2\pi/\lambda$, is the radian frequency and $A$ is an arbitrary complex

constant; c.c. denotes complex conjugate. The characteristic equation for the symmetric-mode complex frequency is derived by substituting (3.2) into (3.1):

$$\omega^2(1+\mu q\tanh q)+2\omega[-kS+\mathrm{i}(f+gq\tanh q)]-(1+Bk^4)q\tanh q+(kS)^2-2\mathrm{i}fkS=0, \tag{3.3}$$

where $q$ is defined by

$$q^2=k^2-Q^2(\omega-kS)^2. \tag{3.4}$$

We investigate the critical condition of neutral stability by setting $\mathrm{Im}\,(\omega)=0$ and separating (3.3) into its real and imaginary parts:

$$\omega^2(1+\mu q\tanh q)-2\omega(kS)-(1+Bk^4)q\tanh q+(kS)^2=0, \tag{3.5a}$$

$$\omega(\gamma+\mu q\tanh q)-\gamma kS=0, \tag{3.5b}$$

where $\gamma=f^*/g^*$ is the ratio of fluid damping to wall damping. We will find that these two damping effects only appear as a ratio. In the case of $Q=0$ we see that $q=k$, and (3.5$a$, $b$) readily uncouple to solve for the fluid speed $S(k)$ and the real frequency $\omega(k)$ as in Grotberg & Reiss (1984). For $Q\neq 0$, however, (3.5) are mixed algebraic–transcendental forms. If we could find $S(k)$ explicitly for $Q\neq 0$ we would seek its minimum value with respect to $k$ and define it as the critical flutter velocity $S_0\equiv S(k_0)$, where $k_0$ is the critical wavenumber. The corresponding critical flutter frequency is $\omega_0\equiv\omega(k_0)$. Alternatively, we take the derivatives of (3.5$a$,$b$) with respect to $k$ and set $(\partial S/\partial k)_{k=k_0}=0$. The two resulting equations are

$$2\omega\frac{\partial\omega}{\partial k}(1+\mu q\tanh q)+\frac{\partial q}{\partial k}\left(\tanh q+\frac{q}{\cosh^2 q}\right)(\mu\omega^2-1-Bk^4)$$
$$-2\left(\frac{\partial\omega}{\partial k}kS+\omega S\right)-4Bk^3q\tanh q+2kS^2=0, \tag{3.5c}$$

$$\frac{\partial\omega}{\partial k}(\gamma+\mu q\tanh q)+\mu\omega\frac{\partial q}{\partial k}\left(\tanh q+\frac{q}{\cosh^2 q}\right)-\gamma S=0, \tag{3.5d}$$

and along with (3.5$a$,$b$) form a system of four equations in four unknowns: $\omega_0$, $k_0$, $S_0$ and $(\partial\omega/\partial k)_{k=k_0}$. By using the known solution for $Q=0$, an iterative numerical scheme readily solves this problem for arbitrary $Q$. A similar process achieves the solution for the antisymmetric mode, where (2.2$b$) is imposed. The corresponding unknown quantities are denoted by $\bar{\omega}_0$, $\bar{k}_0$, $\bar{S}_0$ and $(\partial\bar{\omega}/\partial\bar{k})_{\bar{k}=\bar{k}_0}$.

We note here that a computational error appears in the incompressible analysis of Grotberg & Reiss (1984) for the antisymmetric mode. In that paper the parameter $\bar{\alpha}$ appears in (6.1), but is incorrectly defined. The correct definition is $\bar{\alpha}=\gamma\tanh\bar{k}(\gamma\tanh\bar{k}+\mu\bar{k})^{-1}$. This error leads to some modifications in the $Q=0$ result which will be discussed here.

The results of (3.5) and (3.6) are presented in the next set of figures. In figure 2 we see an example of how the critical flutter speed depends on the damping ratio $\gamma$ for incompressible ($Q=0$) and compressible ($Q=0.5$) flow. In the former case, increasing $\gamma$ has first a stabilizing and then a destabilizing effect as $S_0$ ($\bar{S}_0$) increases and then decreases with a maximum near $\log\gamma=0$. The symmetric mode is always critical for this choice of parameters. In the latter case, the progression is again one of stabilization followed by destabilization, with a shift in the maximum to the right. However, compressibility causes a lowering of the critical velocity in this parameter range (we will see later that this is not always true). As $\gamma$ becomes very large the

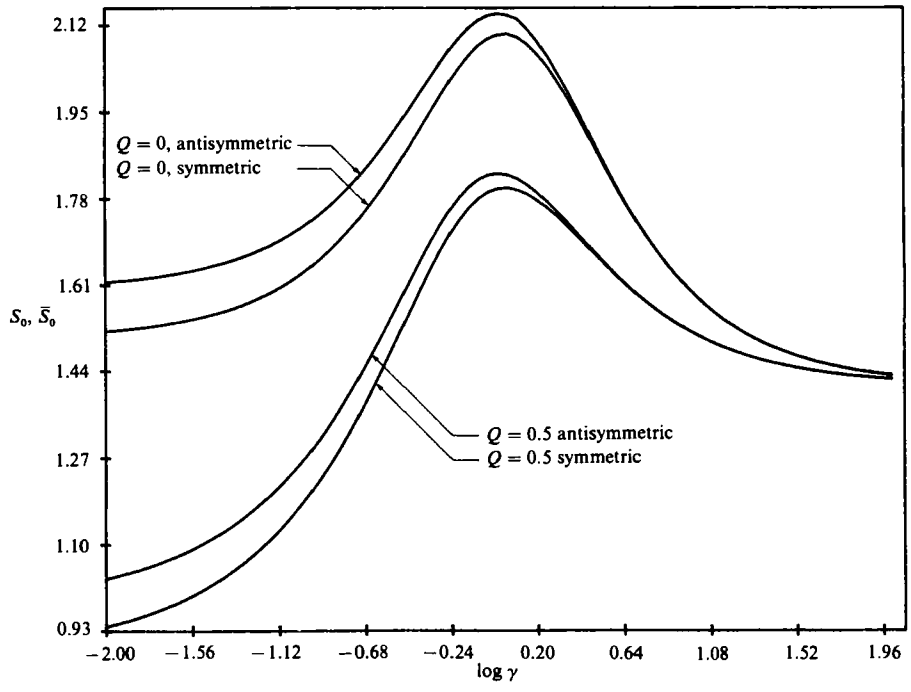


FIGURE 2. Critical flutter speeds $S_0$ and $\bar{S}_0$ versus $\log\gamma$ for $Q = 0$ and 0.5. The remaining parameter values are $\mu = 1$, $B = 1$.

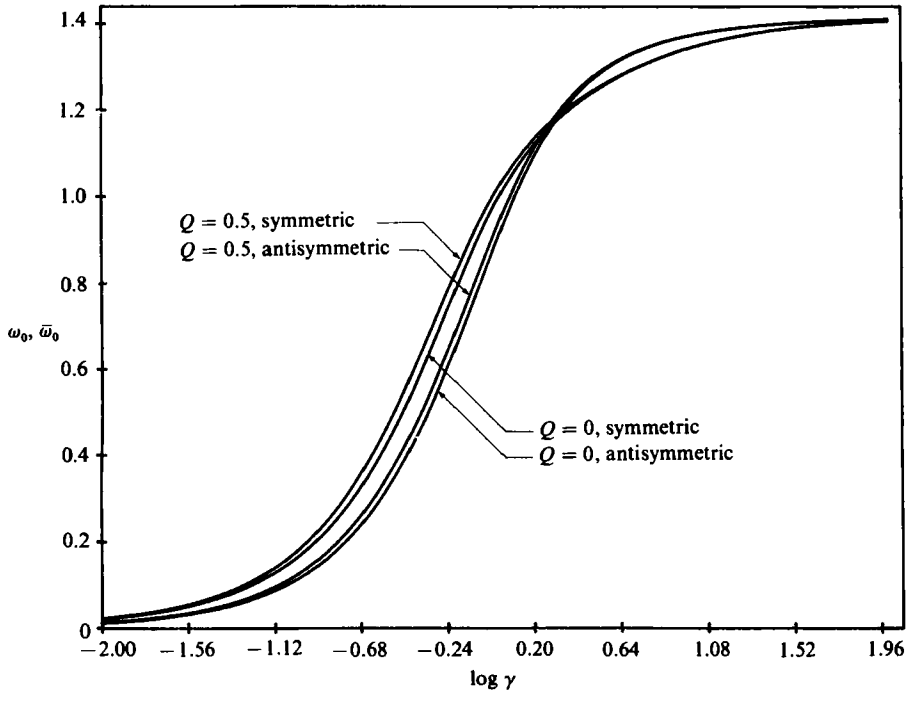


FIGURE 3. Critical flutter frequencies $\omega_0$ and $\bar{\omega}_0$ versus $\log\gamma$ for $Q = 0$ and 0.5. The remaining parameter values are $\mu = 1$, $B = 1$.

solutions for $Q = 0.5$ approach a common limit $S_0$ ($\overline{S}_0$) = 1.40, which is not seen for $\overline{S}_0$ in Grotberg & Reiss owing to the error.

Figure 3 displays the dependence of the critical flutter frequency on $\gamma$ for $Q = 0, 0.5$. We note that this unstable wave is travelling in the downstream direction. The frequencies are monotonically increasing with a common asymptote of 1.4 as $\gamma \to \infty$ (not seen for $\overline{S}_0$ in Grotberg & Reiss) and an asymptote of zero as $\gamma \to 0$. That is, the absence of fluid damping results in a static divergence instability, which is consistent with the previous inviscid models of Matsuzaki & Fung (1977) and Weaver & Paidoussis (1977). Compressibility clearly increases the flutter frequency for any given value of $\gamma$. This result is not immediately intuitive, since a compressible fluid could be thought of as contributing to a less-stiff system. Apparently, the downstream wall wave is less impeded by a more deformable fluid, and consequently attains higher speeds.

Figure 4(*a*) shows the variation of $S_0$ ($\overline{S}_0$) with the mass ratio $\mu$, which is monotonically decreasing. However, a region of the $\log\mu$ axis is magnified in figure 4(*b*), where we see that the antisymmetric mode is critical for lower values of $\mu$, while the symmetric mode becomes critical for higher values. This crossover occurs at $\log\mu = -1.104$ for $Q = 0$ and at $\log\mu = -1.025$ for $Q = 0.5$. The effect of compressibility is to increase the flutter speeds when the symmetric mode is critical and to decrease the flutter speeds when the antisymmetric mode is critical. In figure 5 the flutter frequency monotonically decreases with increasing wall mass as one would expect (not seen for $\overline{\omega}_0$ in Grotberg & Reiss). The fluid compressibility raises the frequencies. Figure 6 isolates the compressibility effects on $S_0$ ($\overline{S}_0$) as we fix all other parameters and vary only $Q$. As $Q$ increases, there can be two qualitatively different results depending on the size of $\gamma$. For $\gamma = 1$ the critical speeds are monotonically decreasing, with the symmetric mode critical. For $\gamma = 0.1$, however, increasing $Q$ first lowers $S_0$, and then raises it until it intersects $\overline{S}_0$ at $\log Q = 0.5$. At that point the antisymmetric mode is critical, and further increases in $Q$ cause $S_0$ to decrease and then increase monotonically. Hence compressibility plays a dual role (not seen in figure 2), which may be masked into a single role if the fluid damping is large enough. The effects on $\omega_0$ ($\overline{\omega}_0$) in figure 7 are monotonically increasing.

## 4. Nonlinear stability theory

To investigate the nonlinear stability of this channel-flow problem we employ the Poincaré–Linstedt method to analyse the system for fluid speeds near the bifurcation point $S_0$ ($\overline{S}_0$). Our intent is to relate the amplitude of the motion to the flow speed and flutter frequency and to see how fluid compressibility influences both. First we define the timescale $\tau$ by

$$\tau \equiv \omega t, \tag{4.1}$$

and a small amplitude parameter $\epsilon$ by

$$\epsilon^2 \equiv \langle \boldsymbol{\Psi} - \boldsymbol{\Psi}_0, \boldsymbol{\Psi} - \boldsymbol{\Psi}_0 \rangle, \tag{4.2}$$

where $\boldsymbol{\Psi}_0$ is the basic-state plug flow represented in our vector notation of §3:

$$\boldsymbol{\Psi}_0 = \begin{bmatrix} Sx \\ -1 \\ Sx \end{bmatrix}. \tag{4.3}$$

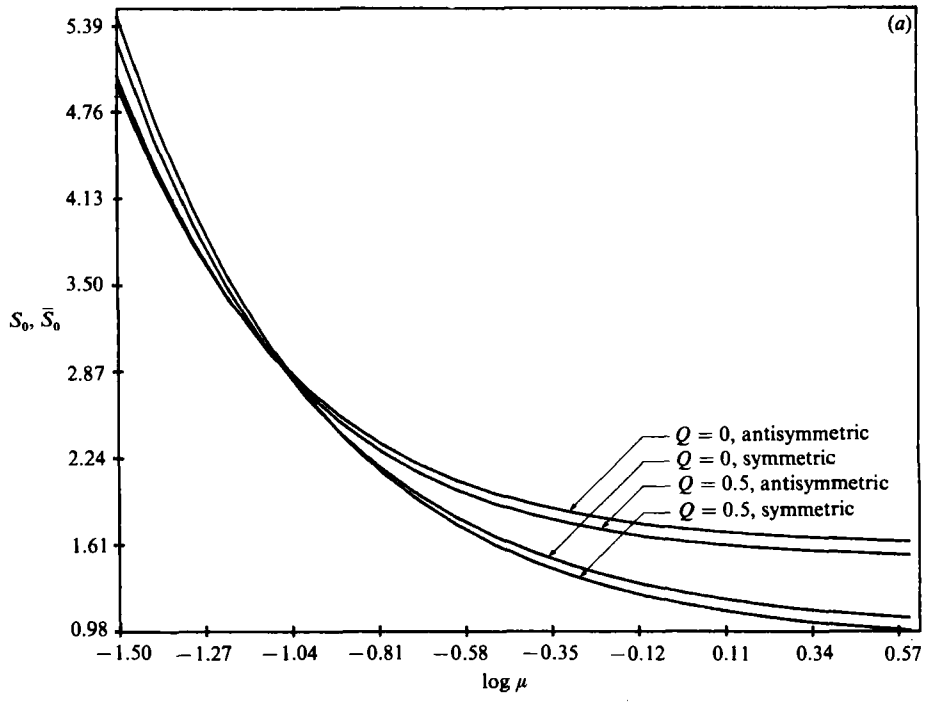


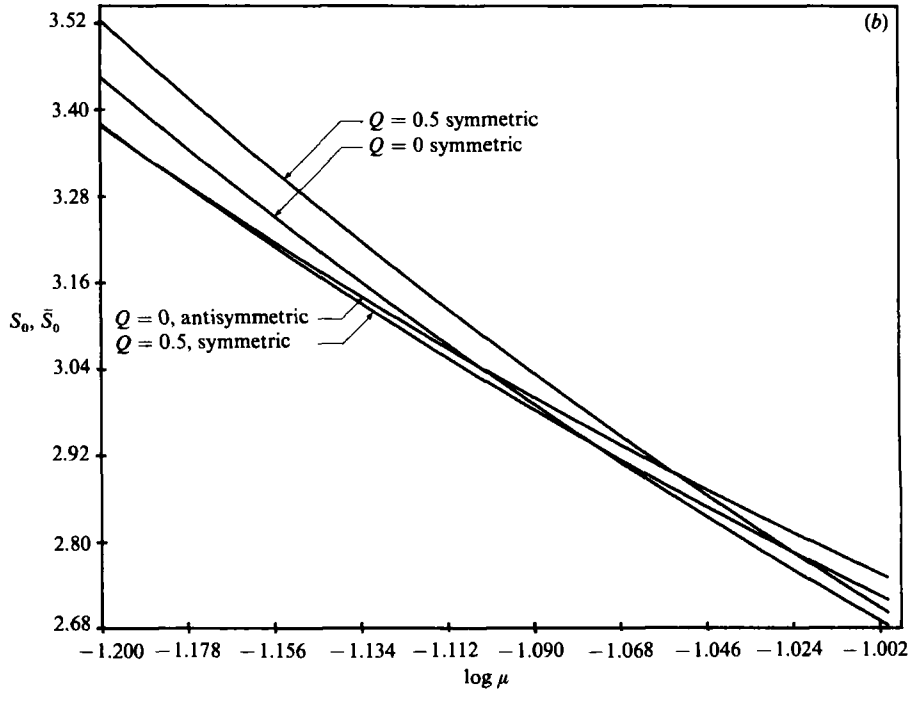


FIGURE 4. (*a*) Critical flutter speeds $S_0$ and $\bar{S}_0$ versus $\log\mu$ for $Q = 0$ and 0.5. The remaining parameter values are $\gamma = 1$, $B = 1$. (*b*) A magnified portion of (*a*) showing exchange of critical modes.

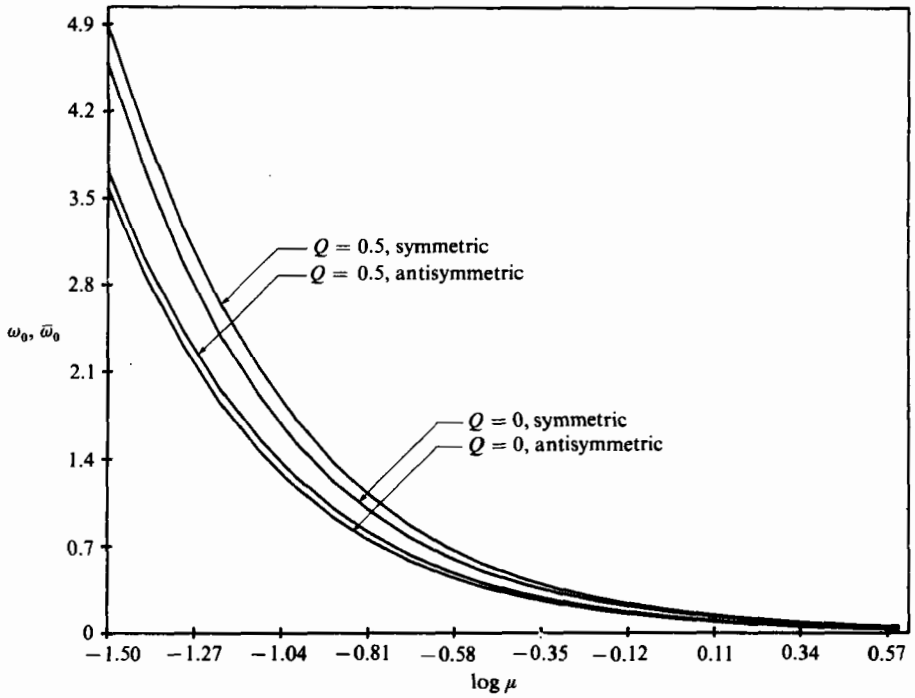


FIGURE 5. Critical flutter frequencies $\omega_0$ and $\bar{\omega}_0$ versus $\log\mu$ for $Q = 0$ and 0.5. The remaining parameter values are $\gamma = 1$, $B = 1$.

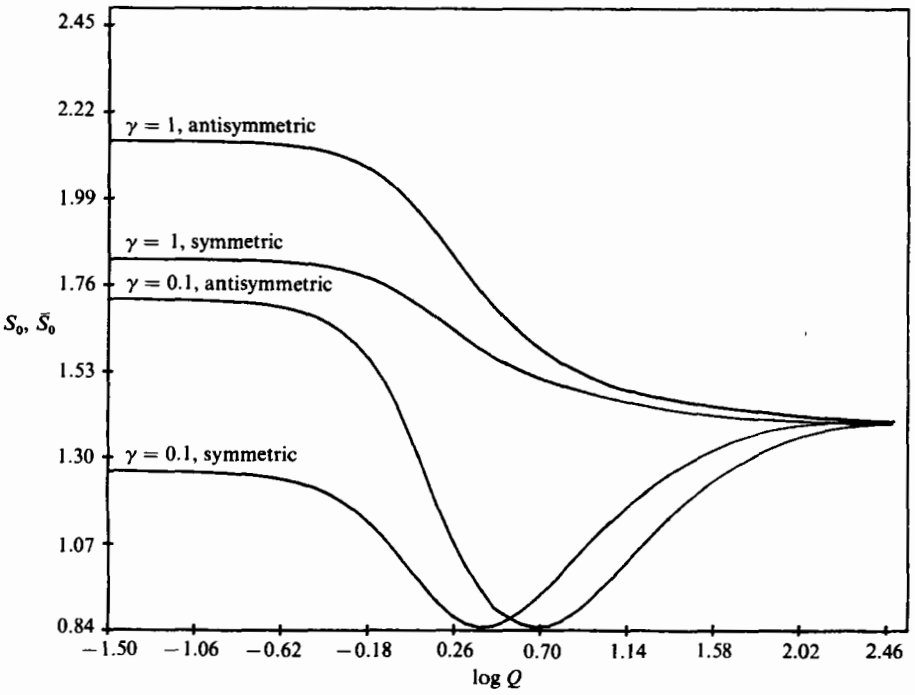


FIGURE 6. Critical flutter speeds $S_0$ and $\bar{S}_0$ versus $\log Q$ for $\gamma = 1$ and 0.1. The remaining parameter values are $\mu = 1$, $B = 1$.

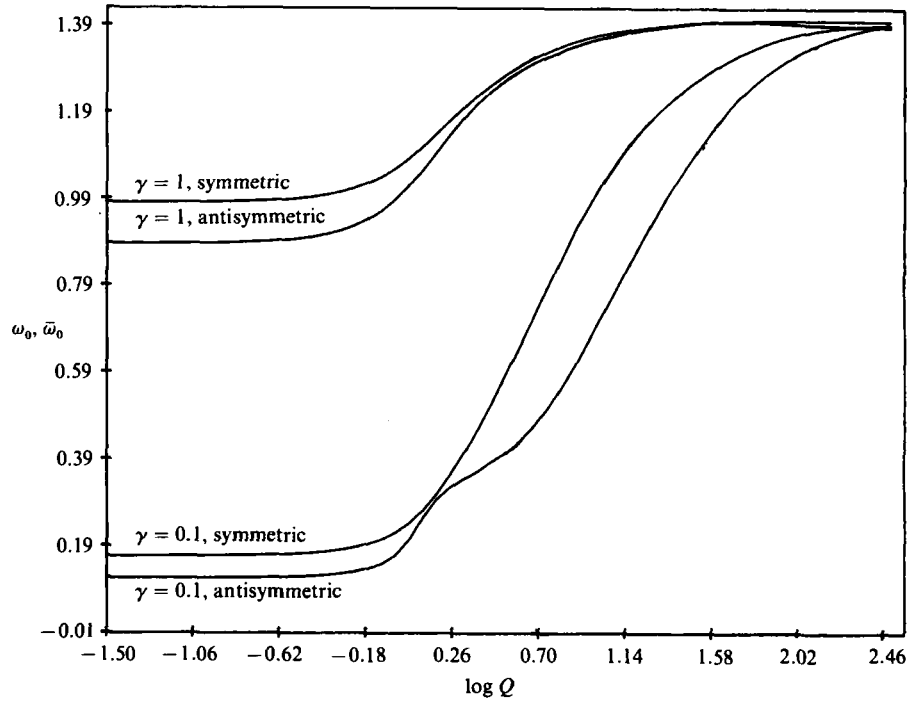


FIGURE 7. Critical flutter frequencies $\omega_0$ and $\bar{\omega}_0$ versus $\log Q$ for $\gamma = 1$ and 0.1. The remaining parameter values are $\mu = 1$, $B = 1$.

The angular brackets in (4.2) denote an inner product given by

$$\langle f, g \rangle = k_0 \int_\tau^{\tau+2\pi} \int_x^{x+2\pi/k_0} \int_0^{-1} (f \cdot g)\, dz\, dx\, d\tau \tag{4.4}$$

for any two vectors $f$ and $g$ that are periodic in $x$ and $\tau$. We examine this governing equation in the neighbourhood of $S_0$ by expanding the dependent variables in powers of the small amplitude parameter,

$$\Psi = \Psi_0 + \epsilon\Psi_1 + \epsilon^2\Psi_2 + \epsilon^3\Psi_3 + \ldots, \tag{4.5a}$$

$$\omega = \omega_0 + \epsilon\omega_1 + \epsilon^2\omega_2 + \ldots, \tag{4.5b}$$

$$S = S_0 + \epsilon S_1 + \epsilon^2 S_2 + \ldots, \tag{4.5c}$$

and inserting these expansions into (2.1)–(2.5). By ordering the resulting equations in powers of $\epsilon$, a sequence of linear problems is found which will determine the unknown coefficients in (4.5$b$, $c$) and the unknown functions in (4.5$a$).

To leading order, the plug-flow solution $\Psi_0$ is given in (4.3), while at $O(\epsilon)$ the linear solutions $\Psi_1$, $\omega_0$ and $S_0$ have already been discussed. At $O(\epsilon^2)$ the resulting governing equations have the form

$$\mathbf{L} \cdot \Psi_2 = F_2 + S_1 G_1 + \omega_1 H_1 = R_2, \tag{4.6}$$

where the vector functions $\boldsymbol{F}_2$, $\boldsymbol{G}_1$ and $\boldsymbol{H}_1$ are given by

$$\boldsymbol{G}_1 = \begin{bmatrix} 2Q^2(\omega_0 \Phi_{1\tau x} + S_0 \Phi_{1xx}) \\ -\Phi_{1x} \\ W_{1x} \end{bmatrix}, \quad \boldsymbol{H}_1 = \begin{bmatrix} 2Q^2(\omega_0 \Phi_{1\tau\tau} + S_0 \Phi_{1\tau x}) \\ 2\mu\omega_0 W_{1\tau\tau} + 2gW_{1\tau} - \Phi_{1\tau} \\ W_{1\tau} \end{bmatrix}, \tag{4.7a, b}$$

$$\boldsymbol{F}_2 = \begin{bmatrix} 0 \\ -\tfrac{1}{2}(\Phi_{1x}^2 + \Phi_{1z}^2) - W_1(\omega_0 \Phi_{1\tau z} + S_0 \Phi_{1xz} + 2f\Phi_1) \\ W_{1x}\Phi_{1x} - W_1 \Phi_{1zz} \end{bmatrix}. \tag{4.7c}$$

The homogeneous problem corresponding to (4.6) has a non-zero solution, as we have already seen. Consequently, solutions exist to the non-homogeneous problem if the right-hand side of (4.6) is orthogonal to the null space of the adjoint operator $\mathbf{L}^*$. This operator and its two-dimensional null-space vectors $\boldsymbol{\Psi}_1^*$ and $\boldsymbol{\Psi}_2^*$ are derived in Appendix A. The solvability condition is then given by the inner-product notation

$$\langle \boldsymbol{R}_2, \boldsymbol{\Psi}_1^* \rangle = 0, \quad \langle \boldsymbol{R}_2, \boldsymbol{\Psi}_2^* \rangle = 0. \tag{4.8}$$

It is readily deduced from (4.8) that

$$\omega_1 = S_1 = 0; \tag{4.9}$$

that is, the first corrections to the flutter speed and flutter frequency are zero. The particular solution to (4.6) is found by determining $\boldsymbol{F}_2$ from $\boldsymbol{\Psi}_1$ and using the method of undetermined coefficients.

At $O(\epsilon^3)$ the above process is repeated, and the governing system has the form

$$\mathbf{L} \cdot \boldsymbol{\Psi}_3 = \boldsymbol{F}_3 + S_2 \boldsymbol{G}_1 + \omega_2 \boldsymbol{H}_1 = \boldsymbol{R}_3, \tag{4.10}$$

where $\boldsymbol{G}_1$ and $\boldsymbol{H}_1$ are given in (4.7*a*, *b*) and $\boldsymbol{F}_3$ is simplified for structural nonlinearity much larger than fluid nonlinearity:

$$\boldsymbol{F}_3 \sim \begin{bmatrix} 0 \\ -dW_{1xx} \displaystyle\int_x^{x+\lambda} (W_{1x})^2 \, \mathrm{d}x \\ 0 \end{bmatrix}. \tag{4.11}$$

The solvability conditions (4.8) applied to $\boldsymbol{R}_3$ yield the next corrections for $\omega_2$ and $S_2$, which are

$$S_2 = \frac{-2\lambda_0 d k_0^4 A^2 A_{22}}{A_{11}A_{22} - A_{12}A_{21}} > 0, \quad \omega_2 = \frac{-S_2 A_{21}}{A_{22}} > 0. \tag{4.12a, b}$$

The matrix components $A_{ij}$ $(i,j = 1,2)$ are defined by

$$\left.\begin{aligned} A_{11} &= -2mk_0J^3 - \frac{2k_0J}{q_0\tanh q_0}, \quad A_{12} = 2mJ^3 + \frac{2J}{q_0\tanh q_0} - 2\omega_0\mu, \\ A_{21} &= 4mfk_0J^2 + \frac{2fk_0}{q_0\tanh q_0}, \quad A_{22} = -4mfJ^2 - 2\left(g + \frac{f}{q_0\tanh q_0}\right), \end{aligned}\right\} \tag{4.13}$$

where

$$\left.\begin{aligned} m &= \frac{Q^2}{q_0^2\sinh^2 q_0}\left(\frac{1}{2} + \frac{1}{4q_0}\sinh 2q_0\right), \\ J &= k_0S_0 - \omega_0. \end{aligned}\right\} \tag{4.14}$$

The system bifurcates supercritically since $S_2 > 0$, and it stiffens, $\omega_2 > 0$, as the fluid speed is increased beyond $S_0$. This is similar to the incompressible case; however, we would like to know how compressibility affects the amplitude and frequency of the nonlinear state. By rearranging (4.5*c*), we solve for the amplitude $\epsilon$,

$$\epsilon = \left(\frac{S - S_0}{S_2}\right)^{\frac{1}{2}}, \tag{4.15}$$

and see that it is inversely related to $S_2^{\frac{1}{2}}$. Except for the parameter $d$, each term in (4.12*a*) depends on $Q$. In particular, the linear amplitude $A^2$ is determined from the definition (4.2) and found to be

$$A^2 = \frac{1}{2}\left[\left(1 + \frac{\sinh 2q_0}{2q_0} + 2\cosh^2 q_0\right)\frac{J^2}{2q_0^2\sinh^2 q_0} + 1\right]^{-1}. \tag{4.16}$$

The entire nonlinear analysis may be repeated to determine the antisymmetric-mode counterparts to (4.5). The variation of $S_2$ and $\overline{S}_2$ with $Q$ is given in figure 8 and seen to be monotonically decreasing with increasing $Q$. Hence the amplitude of the motion becomes larger as the fluid becomes more compressible. The more-deformable fluid allows the walls to deform to a greater degree. The effect is somewhat larger for the antisymmetric mode near $\log Q = 0$, where the decrease in $\overline{S}_2$ occurs much more rapidly than $S_2$. The correction to the flutter frequency is shown in figure 9, where $\omega_2$ and $\overline{\omega}_2$ are plotted as functions of $Q$; the stiffening effect at first becomes larger as $Q$ increases, while the opposite occurs for the higher $Q$-values.

## 5. Stability of the flutter states

To test the stability of the supercritical bifurcation we examine the initial-value problem for $S - S_0$ small and positive by employing the two-time method. Thus we intend to analyse the growth of oscillations to a limit cycle whose long-time solution coincides with the frequency and amplitude found in §4. We define the distance from $S_0$ by

$$S = S_0 + \delta^2, \tag{5.1}$$

where $\delta$ is small, and relate this parameter to the growth rate of oscillation amplitude. This growth rate is scaled as the slow time

$$T \equiv \delta^2 t, \tag{5.2}$$

and we assume that the initial disturbance at time $t = 0$ is periodic and small, of order $\delta$.

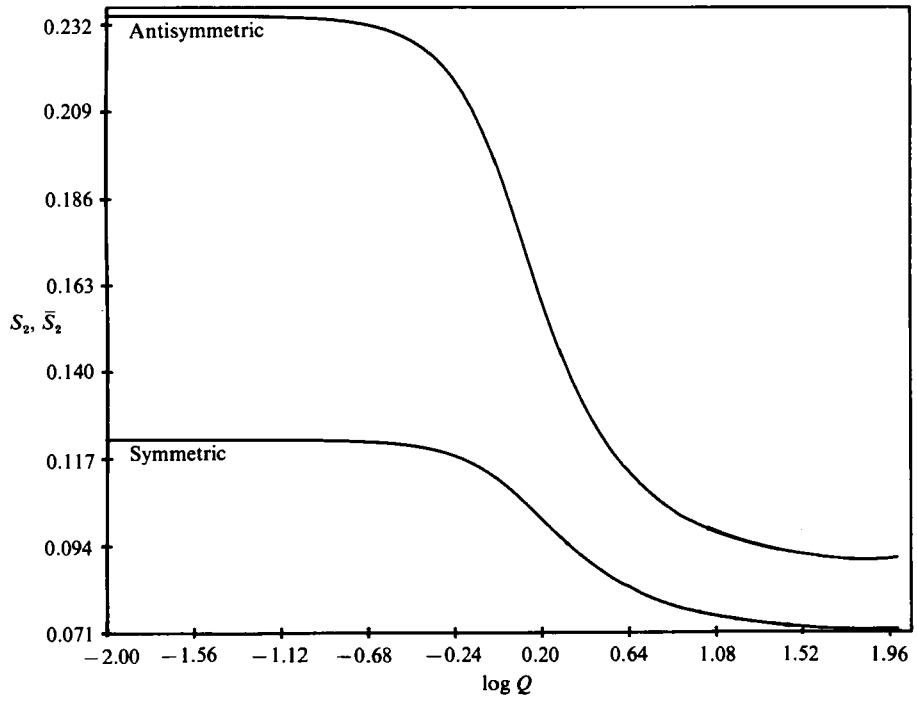


FIGURE 8. The nonlinear correction to the critical flutter speeds $S_2$ and $\bar{S}_2$ versus $\log Q$ for $\gamma = 1$, $\mu = 1$, $B = 1$.

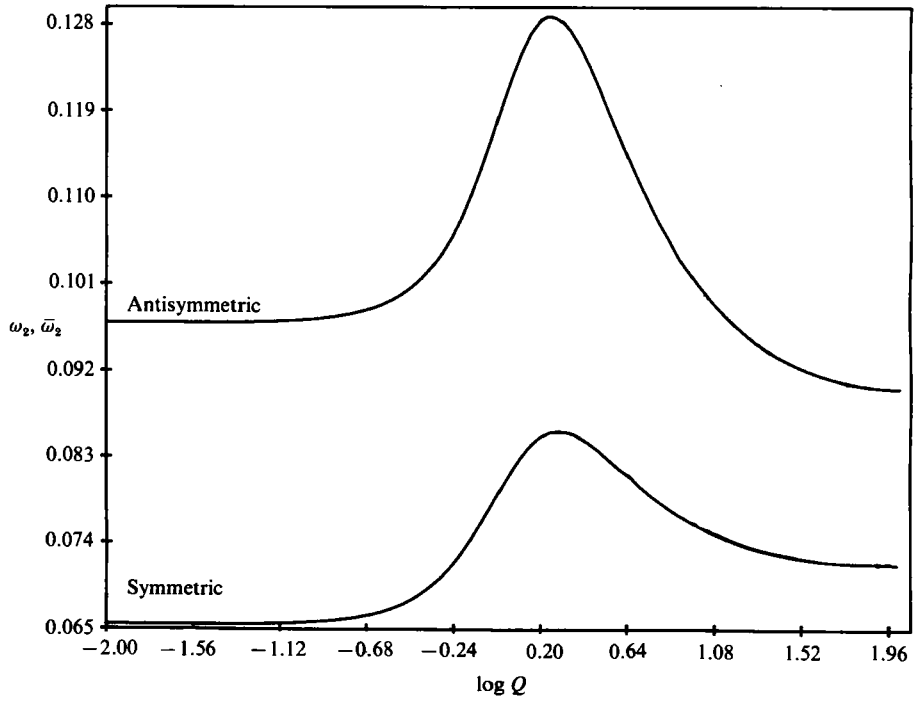


FIGURE 9. The nonlinear correction to the critical flutter frequencies $\omega_2$ and $\bar{\omega}_2$ versus $\log Q$ for $\gamma = 1$, $\mu = 1$, $B = 1$.

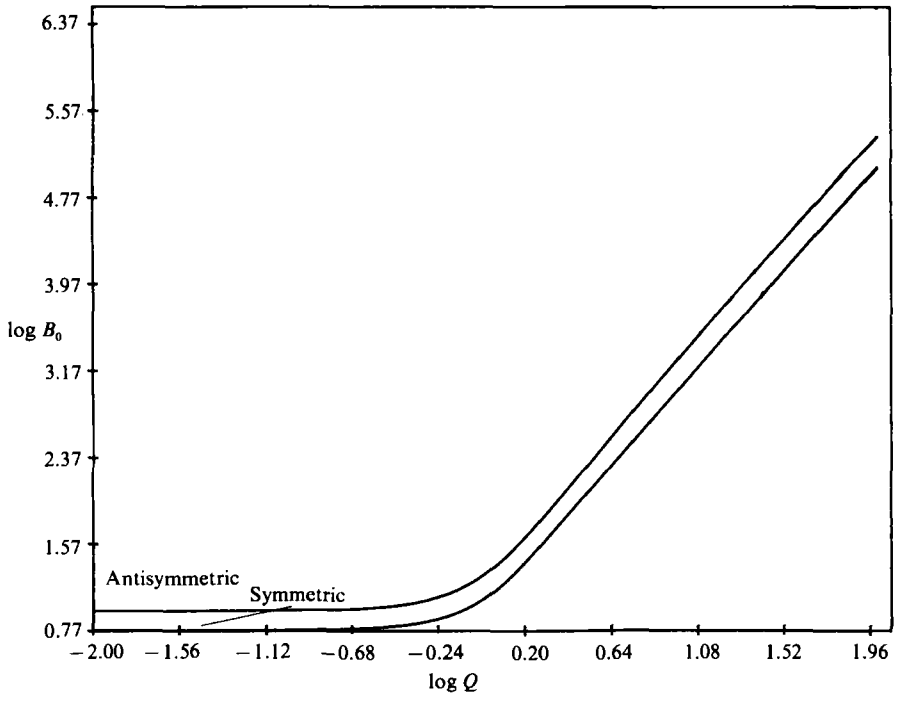


FIGURE 10. The growth rate of unstable oscillations to a stable limit cycle $\log B_0$ versus $\log Q$ for $\gamma = 1$, $\mu = 1$, $B = 1$.

We proceed as outlined in Grotberg & Reiss (1984) by expanding the dependent variables in powers of $\delta$ and solving a sequence of linear problems which lead to a nonlinear ordinary differential equation for the complex amplitude $A_1(T)$:

$$aA_{1T} + bA_1 + c\bar{A}_1 A_1^2 = 0. \tag{5.3}$$

The complex coefficients are related to (4.13), while the real coefficient $c$ depends on $d$:

$$a = -A_{22} + iA_{12}, \quad b = A_{11} + iA_{21}, \quad c = 2\lambda d k^4. \tag{5.4a, b, c}$$

To solve (5.3) it is convenient to express $A_1(T)$ in polar form:

$$A_1(T) = p(T)\, e^{iq(T)}, \tag{5.5}$$

where the growth rate $p(T)$ and the frequency shift $q(T)$ are both real functions. When (5.5) is inserted into (5.3), the resulting complex equation may be separated into real and imaginary parts. By eliminating $q$, we arrive at the equation for $p$:

$$A_0 p_T - B_0 p + C_0 p^3 = 0. \tag{5.6}$$

The coefficients are defined by

$$A_0 = A_{22}^2 + A_{12}^2 > 0, \quad B_0 = A_{11} A_{22} - A_{12} A_{21} > 0, \quad C_0 = -A_{22} c.$$

Equation (5.6) may be separated and integrated. The solution is found to be

$$p^2 = \frac{-B_0 K e^{2B_0 T/A_0}}{1 - C_0 K e^{2B_0 T/A_0}}, \tag{5.7}$$

where $K$ depends on the initial value $p(0) \equiv p_0$:

$$K = \frac{P_0^2}{-B_0 + C_0 P_0^2}. \tag{5.8}$$

The growth rate of amplitude is proportional to $B_0 \delta^2$. For a given $\delta$, the fluid compressibility will change the growth rate of the oscillations by modifying $B_0$, shown in figure 10. As $Q$ increases from zero the growth rate increases monotonically, with a very rapid increase starting near $\log Q = 0$. Note that the vertical axis is also logarithmic.

## 6. The frictionless system: a singular limit

In many theories of flutter phenomena, both fluid and wall properties are chosen to exclude friction. In the present analysis we can examine these cases by setting $f = 0$, $g = 0$ in (3.3). Since $q$ is either real or pure imaginary the product $q \tanh q$ is always real, and (3.3) becomes a real quadratic for $\omega$:

$$\omega = \frac{ks \pm [(1+\mu q \tanh q)(1+Bk^4) q \tanh q - \mu q \tanh q (kS)^2]^{\frac{1}{2}}}{1+\mu q \tanh q}, \tag{6.1}$$

which has two solutions in general. The stability boundary is found by setting the bracketed term to zero and solving for the critical speed $S_0$. The corresponding solution of $\omega_0$ in (6.1) is only single-valued at the critical speed:

$$\omega_0 = \frac{kS_0}{1+\mu q \tanh q}; \tag{6.2}$$

that is, the eigenvalues coalesce at criticality, unlike the frictional system. The implication of this coalescence is clearly seen when $S$ is increased beyond $S_0$ and we seek the nonlinear solution. From (4.13) we see that $A_{21} = A_{22} = 0$ in the frictionless case, so that the matrix equation used to solve for $\omega_i$, $S_i$ $(i = 1, 2)$ in (4.5*b*, *c*),

$$\begin{bmatrix} A_{11} & A_{12} \\ A_{21} & A_{22} \end{bmatrix} \begin{bmatrix} \omega_i \\ S_i \end{bmatrix} = \boldsymbol{T}_i, \tag{6.3}$$

is singular. Consequently, in a frictionless system the branch of solutions bifurcating from $S = S_0$ cannot be uniquely determined, since the $\omega_i$ and $S_i$ are linearly related, with one of them arbitrary. This differs significantly from the frictional system, which is uniquely determined, as we have seen. So when the null space of the linear operator reduces from two dimensions to one dimension (eigenvalue coalescence) the resulting singularity leads to a non-unique solution. Of course, in any experiment we have friction and observable bifurcation states that are not arbitrary, so the frictionless system is a poor analogue of flutter phenomena.

## 7. The hydraulic approximation as a limit of the Orr–Sommerfeld system

The hydraulic approximation used in this analysis leads to a stability theory which predicts flutter oscillations in flow through a flexible channel. The theory excludes the possibility of fluid instabilities, so it does not represent a modification of Tollmien–Schlichting waves. However, we now demonstrate that this theory is a

particular limiting form of the full viscous equations, so that it can be related to the Orr–Sommerfeld system. To show the analogy, we consider the disturbance stream function for incompressible flow, $\psi = \phi(z)\, e^{ik(x-ct)}$, which is related to the disturbance velocities by $(u, v) = (\psi_z, -\psi_x)$. If the basic-state channel-flow velocity profile is $\bar{u}(z)$ then the familiar form of the linearized stream-function equation is

$$\frac{i\epsilon^2}{k} L^2\phi + (\bar{u}-c)\, L\phi = \bar{u}_{zz}\,\phi. \tag{7.1}$$

The linear operator $L \equiv d^2/dz^2 - k^2$ and the parameter $\epsilon^2 \equiv R^{-1}$, where $R$ is the Reynolds number. We let the velocity be scaled on $C = (E/\rho_f)^{\frac{1}{2}}$ and define $R = bC/\nu$. If a basic-state plug flow is assumed then $\bar{u} = S$, and in the limit $\epsilon^2 \to 0$, (7.1) simplifies to

$$(S-c)\, L\phi = 0, \tag{7.2}$$

subject to inviscid boundary conditions. For example, the symmetric-mode eigenfunction must satisfy the midline condition $\psi(0) = 0$, and is readily found to be

$$\phi = \sinh kz \tag{7.3}$$

for $S \neq c$. The kinematic boundary condition of no cross-flow at the lower wall, $z = -1 + \eta\, e^{ik(x-ct)}$, has the form

$$(S-c)\,\eta = -\phi \quad (z = -1). \tag{7.4}$$

By balancing the full viscous and pressure forces with the plate response, the normal component of the plate equation can be shown to be

$$(-(kc)^2\mu - 2ikcG + Bk^4 + 1)\,\eta - (S-c)\,\phi_z - \frac{i}{k}\epsilon^2(\phi_{zzz} - 3k^2\phi_z) = 0 \quad (z = 1), \tag{7.5}$$

where the coefficient of $\eta$ is the familiar plate response, the middle term is the inviscid pressure and the coefficient of $\epsilon^2$ represents the viscous pressure and normal stress. We insert (7.3) and (7.4) into (7.5) and examine the stability boundary by setting $\mathrm{Im}\,(c) = 0$. Before taking the limit of $\epsilon^2 \to 0$, we separate (7.5) into its real and imaginary parts:

$$c^2(1 + \mu k \tanh k)\, k - 2ckS - (1 + Bk^4)\tanh k + kS^2 = 0, \tag{7.6a}$$

$$cGk \tanh k - \epsilon^2 k^2 (S-c) = 0. \tag{7.6b}$$

We let the plate damping $G = \Gamma\epsilon^n$ and consider the limit of (7.6$b$) as $\epsilon$ approaches zero:

$$c\Gamma k \tanh k = \lim_{\epsilon \to 0} \epsilon^{2-n}(S-c). \tag{7.7}$$

For $n < 2$ the limit gives the static divergence result $c = 0$ whenever $\Gamma \neq 0$. This is similar to the previous theories (Matsuzaki & Fung 1977, 1978; Weaver & Paidoussis 1977), which use inviscid-flow theory and damped walls. From (7.6$a$) the divergence velocity is found to be

$$S_D = \left[\frac{(1 + Bk^4)\tanh k}{k}\right]^{\frac{1}{2}}. \tag{7.8}$$

If $n > 2$ then $S-c = 0$, which is not permitted in (7.2). However, if $n = 2$ then both terms in (7.7) balance. This limit may be interpreted on a physical basis as one in which the fluid viscosity, though small, is comparable to the wall viscosity as $\epsilon^2 \to 0$. Since the inviscid eigenfunction (7.3) is used we see that the boundary layer is thin enough that, to leading order, it does not influence the flow field but does dictate the plate instability to be flutter, $c \neq 0$, instead of static divergence. Indeed, by defining $\Gamma = \mu k^2/\gamma$, (7.6*a*, *b*) reduce to the flutter instability criteria found in Grotberg & Reiss (1984) and the present paper for $Q = 0$:

$$c = \alpha S, \quad S = \left[\frac{(1+Bk^4)\tanh k}{\alpha^2 \mu k \tanh k + (1-\alpha)^2}\right]^{\frac{1}{2}},$$

where $\alpha = \gamma(\gamma + \mu k \tanh k)^{-1}$. The linear stability of the hydraulic approximation and this limit of the full equations are identical, and one can see that their respective nonlinear stabilities are also the same, since the viscous terms are all linear. The hydraulic approximation differs from this limit in the basic state, since the former yields a constant pressure gradient and the latter does not. The external plate conditions were chosen to cancel the effects of any internal pressure gradient as the basic channel shape of parallel plates, so this does not present a difficulty for the stability problem.

## 8. Conclusions

In the present analysis we have examined the stability of compressible flow through a two-dimensional flexible channel. In general, the presence of fluid damping leads to flutter instability in the symmetric (antisymmetric) mode at a critical speed $S_0$ ($\overline{S}_0$) with frequency $\omega_0$ ($\overline{\omega}_0$). Fluid compressibility causes increases or decreases in $S_0$ ($\overline{S}_0$) and can change the instability from one mode to the other. However, $\omega_0$ ($\overline{\omega}_0$) monotonically increases with compressibility, since the more deformable fluid is less resistant to the wall wave. In the nonlinear theory we found that this greater deformability leads to larger-amplitude motions, which have faster growth rates to the limit cycle. In addition, the limit of a frictionless system proved to be singular in that the nonlinear state is not uniquely determined. The hydraulic approximation incorporated in the analysis is a particular limit of the full Orr–Sommerfeld system.

This research was supported by the National Science Foundation Presidential Young Investigator Award in conjunction with General Motors Corporation and The Whitaker Foundation.

## Appendix A

The linear operator $\mathbf{L}$ and its adjoint operator $\mathbf{L}^*$ have the relation

$$\langle \boldsymbol{\Psi}_i, \mathbf{L}\cdot\boldsymbol{\Psi}_j \rangle = \langle \boldsymbol{\Psi}_j, \mathbf{L}^*\cdot\boldsymbol{\Psi}_j \rangle,$$

where the angular brackets stand for the inner product

$$\langle \boldsymbol{\Psi}_i, \boldsymbol{\Psi}_j \rangle = \frac{1}{\lambda\tau}\int_t^{t+\tau}\int_x^{x+\lambda}\int_{-1}^{0} \boldsymbol{\Psi}_i\cdot\boldsymbol{\Psi}_j \,\mathrm{d}z\,\mathrm{d}x\,\mathrm{d}t.$$

Through integration by parts, the adjoint operator is found to be

$$\mathbf{L}^* = \begin{bmatrix} \nabla^2 + Q^2\left(\frac{\partial}{\partial t} + S_0\frac{\partial}{\partial x}\right)^2 & 0 & 0 \\ 0 & -\left(\mu\frac{\partial^2}{\partial t^2} - 2g\frac{\partial}{\partial x} + B\frac{\partial^4}{\partial x^4} + 1\right) & \frac{\partial}{\partial t} + S_0\frac{\partial}{\partial x} \\ \frac{\partial}{\partial z}(\quad)_{z=-1} & 2f - \frac{\partial}{\partial t} - S_0\frac{\partial}{\partial x} & 0 \end{bmatrix} \tag{A 1}$$

at $S = S_0$.

The homogeneous adjoint problem for the symmetric mode is

$$\mathbf{L}^* \cdot \boldsymbol{\Psi}^* = \mathbf{0}, \tag{A 2}$$

with the boundary condition $\Phi_z(x, 0, t) = 0$. The null-space solution of (6.2) is two-dimensional, with

$$\begin{aligned} \boldsymbol{\Psi}^* &= \boldsymbol{\Psi}_1^* + \boldsymbol{\Psi}_2^* \\ &= A_1^* \begin{bmatrix} \dfrac{[2f + \mathrm{i}(\omega_0 - k_0 S_0)]\cosh qz}{q \sinh q} \\ \dfrac{2f + \mathrm{i}(\omega_0 - k_0 S_0)}{q \tanh q} \end{bmatrix} \mathrm{e}^{\mathrm{i}\Theta_0} + \text{c.c.}, \end{aligned}$$

where $\Theta_0 = k_0 x - \omega_0 t$. The arbitrary constant $A_1^*$ is complex in general, and thus gives two linearly independent solutions corresponding to the $\mathrm{e}^{\mathrm{i}\Theta_0}$ and the $\mathrm{e}^{-\mathrm{i}\Theta_0}$ terms respectively. We can solve for $\omega_1$ and $S_1$ by the Fredholm alternative (4.8).

## Appendix B

$a$ $\equiv$ local sound speed, $2b \equiv$ channel depth,

$B = \dfrac{D}{Eb^4}$, $C = \left(\dfrac{Eb}{\rho_f}\right)^{\frac{1}{2}}$,

$d = \dfrac{D}{6\lambda^* b^2 h^2 E}$, $D = \dfrac{Yh^3}{12(1-\sigma^2)}$,

$E$ $\equiv$ elastance of spring supports,

$f^*$ $\equiv$ fluid-damping coefficient, $2f = \dfrac{f^* b}{C}$,

$g^*$ $\equiv$ wall-damping coefficient, $2g = \dfrac{g^* \mu b}{C}$,

$h$ $\equiv$ wall thickness, $M \equiv$ Mach number,

$k = \dfrac{2\pi}{\lambda}$, dimensionless wavenumber,

$P = \dfrac{P^*}{\rho_f C^2}$, dimensionless pressure,

$Q = \dfrac{C}{a}$, compressibility parameter,

$S = \dfrac{U}{C}$, dimensionless speed,

$t = \dfrac{Ct^*}{b}$, dimensionless time,

$U \equiv$ uniform fluid speed, $W =$ wall position,

$x = \dfrac{x^*}{b}$, dimensionless position,

$Y \equiv$ elastic modulus,

$\gamma = \dfrac{f^*}{g^*}$, damping ratio,

$\lambda = \dfrac{\lambda^*}{b}$, dimensionless wavelength,

$\mu = \dfrac{\rho_w h}{\rho_f b}$, mass ratio,

$\sigma \equiv$ Poisson's ratio, $\nu \equiv$ kinematic viscosity,

$\rho_w \equiv$ wall density, $\rho_f \equiv$ fluid density,

$\Phi = \dfrac{\Phi^*}{bC}$, dimensionless velocity potential,

$\omega = \dfrac{\omega^* b}{C}$, dimensionless radian frequency.

## REFERENCES


Dowell, E. E. 1967 Nonlinear oscillations of a fluttering plate. II. *AIAA J.* **5**, 1856–1862.

Gavriely, N., Palti, Y., Alroy, G. & Grotberg, J. B. 1984 Measurement and theory of wheezing breath sounds. *J. Appl. Physiol.: Respirat. Environ. Exercise Physiol.* **57**, 481–492.

Grotberg, J. B. & Davis, S. H. 1980 Fluid-dynamic flapping of a collapsible channel: sound generation and flow limitation. *J. Biomech.* **13**, 219–230.

Grotberg, J. B. & Reiss, E. L. 1984 Subsonic flapping flutter. *J. Sound Vib.* **92**, 349–361.

Matsuzaki, Y. & Fung, Y. C. 1977 Stability analysis of straight and buckled two-dimensional channels conveying an incompressible flow. *Trans. ASME* E: *J. Appl. Mech.* **44**, 548–552.

Matsuzaki, Y. & Fung, Y. C. 1979 Nonlinear stability analysis of a two-dimensional model of an elastic tube conveying a compressible flow. *Trans. ASME* E: *J. Appl. Mech.* **46**, 31–36.

Weaver, D. S. & Paidoussis, M. P. 1977 On collapse and flutter phenomena in thin tubes conveying fluid. *J. Sound Vib.* **50**, 117–132.